RESEARCH ARTICLE

Risk Prediction of Gas Hydrate Formation in the Wellbore and Subsea Gathering System of Deep-Water Turbidite Reservoirs: Case Analysis from the South China Sea

Muyin Li[1,*], **Junyi Liu**[1] **and Yifan Xia**[2]

[1] School of Energy Science and Engineering, Henan Polytechnic University, Jiaozuo 454000, China
[2] School of Petroleum Engineering, China University of Petroleum (East China), Qingdao 266580, China

Abstract

The low temperatures in the deepwater area are associated with a high risk of hydrate formation and flowline blockages in the wellbore and pipelines during the long-term development of gas reservoirs. The occurrence of this risk is required to be prevented and controlled to facilitate the safe and efficient development of offshore gas reservoirs. In this study, a numerical model was developed and solved to calculate the temperature and pressure distributions within wellbore and gathering system, and its applicability was evaluated. The comparison with experimental results verifies that the model is appropriate for predicting temperature and pressure distributions in the wellbore and gathering system during gas reservoir production. Simultaneously, the potential section for hydrate formation in the wellbore, flowline, and riser was examined by comparing the phase equilibrium pressure and actual pressure. The investigation results indicate that hydrate formation risks occurs in the wellbore, flowline, and riser after 10, 8, and 8 years of natural gas production, respectively. At these moments, the lengths of the hydrate formation risk sections in the wellbore, flowline, and riser are 49 m, 2500 m, and 9.8 m, respectively. Since then, the length of the hydrate formation risk section has increased with continued gas production operation. Finally, based on the phase equilibrium conditions associated with various methanol concentrations, the methanol injection concentration was optimized to eliminate the risk of hydrate formation. It is indicated by the investigation results that a methanol injection concentration of 7.5% is required to eliminate the risk of hydrate formation in the wellbore and gathering system.

Keywords: offshore oil and gas, turbidite reservoir, gas hydrate, flow assurance, wellbore safety, inhibitor.

1 Introduction

With the gradual depletion of oil and gas resources and increasing extraction challenges, sustaining

Submitted: 28 August 2025
Accepted: 22 October 2025
Published: 29 October 2025

Vol. 1, **No.** 1, 2025.
10.62762/RS.2025.567907

***Corresponding author:**
✉ Muyin Li
livewood1999@163.com

Citation
Li, M., Liu, J., & Xia, Y. (2025). Risk Prediction of Gas Hydrate Formation in the Wellbore and Subsea Gathering System of Deep-Water Turbidite Reservoirs: Case Analysis from the South China Sea. *Reservoir Science*, 1(1), 52–72.

and increasing production is becoming increasingly challenging for most onshore oilfields in China [1–3]. In recent years, China's reliance on overseas oil and gas has steadily increased, resulting in a significant threat to energy supply security [4, 5]. Over the past decade, China's overseas dependence on crude oil increased from 57.2% in 2013 to 74.0% in 2023, while that of natural gas has increased from 28.9% to 47.0% over the same period. From this perspective, expansion into offshore regions, particularly deepwater and ultra-deepwater areas, has become an inevitable trajectory for the future development of China's oil and gas industry [6]. Over 70% of global oil and gas resources are found in oceanic regions, where deepwater areas represent a vital replacement zone for oil and gas production. The potential oil reserves in these deepwater regions worldwide are approximately 100 billion barrels. The South China Sea, a principal accumulation region of China's offshore hydrocarbon resources, holds substantial potential in turbidite reservoirs, positioning it as a critical frontier for future oil and gas production. Turbidite reservoirs in the South China Sea form primarily through gravity-driven turbidity currents from deltaic fronts or shelf margins, depositing stratified sandstone-mudstone sequences that follow the Bouma cycle: coarse basal sands grading upward into finer silts and clays [7]. These are marked by sinuous, sand-rich channels in basins like Qiongdongnan, extending kilometers with thicknesses up to tens of meters [8, 9]. Their reservoir quality excels due to 20–30% porosity and high permeability from well-sorted, coarse grains. Grain-size data shows turbidites richer in coarse particles than surrounding marls, boosting hydrocarbon trapping but creating lateral discontinuities and thin sands that hinder seismic imaging [10]. Northern South China Sea bottom currents rework these deposits, forming hybrid sandy beds with heightened heterogeneity, altering geometries and fluid connectivity [11, 12]. Under low sea-level, cooler conditions like the last glacial period, fine-grained turbidites dominate gentle slopes, while coarse strata in turbidity settings idealize deep-sea oil, gas, and hydrate reservoirs. In Dongsha and Qiongdongnan, faulting, lithofacies shifts, and intrusions amplify production risks, fostering unpredictable pressure-temperature gradients that promote hydrate nucleation in wellbores and subsea systems [13, 14]. In turbidite reservoirs, these coarse-grained sands introduce distinct flow assurance vulnerabilities that are absent in other fine-grained deep-water analogues. Such vulnerabilities include enhanced sand production and the accelerated formation of hydrates, which together increase the likelihood of flow blockage [15]. The high sand content facilitates heterogeneous nucleation on particle surfaces, thereby shortening the induction time and accelerating hydrate formation. Compared with pure water systems, fine sand particles serve as catalytic sites that promote the growth of methane hydrate inclusion complexes [16, 17]. This synergistic effect not only further compromises wellbore stability but also exacerbates the risk of flow blockage in the turbidite reservoirs of the South China Sea.

The South China Sea contains an estimated 19 Tcf of natural gas and 11 billion barrels of proven oil, as reported by the U.S. EIA [18]. The effective development of such huge oil and gas resources can substantially mitigate the domestic supply-demand imbalance for oil and gas. However, the complexity of development environments can significantly increase the likelihood of safety incidents. Effective flow assurance has become one of the critical technical bottlenecks limiting the safe and efficient development of deepwater oil and gas resources [19, 20].

Flow assurance, proposed in the early 1990s, was considered as a technical framework aimed at ensuring the flow safety in pipeline systems. This technology is widely employed to address flow assurance challenges in deepwater oil and gas production, including wax deposition [21], hydrate formation [22], slugging [23], pipeline corrosion [24], scaling [25], and sand erosion [26]. Specifically, the challenges associated with flow assurance in deepwater oil and gas development primarily arise from the following factors. (1) The low-temperature and high-pressure conditions on the seafloor create a highly favorable environment for hydrate formation in wellbores and pipelines. Following nucleation, hydrate particles tend to agglomerate and adhere to the pipeline wall, forming blockages over time. (2) High-viscosity crude oil, owing to its distinct compositional characteristics, is susceptible to wax and asphaltene deposition during pipeline transport. (3) In long-distance subsea pipelines, abnormal internal friction may arise, which can hinder stable flow and compromise transport efficiency. (4) The complex seabed topography can induce slug flow in pipelines, potentially destabilizing pipelines and related components, and leading to gas kick in separator and cavitation in pressurization equipment. (5) Corrosion from gases such as CO_2 and H_2S in production fluids, combined with sand particle erosion, compromises pipeline

integrity and destabilizes associated equipment. This study focuses on the first aforementioned issue, namely hydrate formation within the wellbore or pipeline during the development process. Figure 1 presents a schematic of hydrate formation and accumulation in wellbores and pipelines in deepwater environment. As depicted in Figure 1, seabed ambient temperatures are generally stable at approximately 4°C in the northern South China Sea. If methane is assumed to be the guest molecule in the hydrate structure, the phase equilibrium pressure at this temperature is approximately 3.18 MPa. When the pressure within the wellbore or pipeline exceeds this equilibrium pressure, hydrate formation may be initiated. Interestingly, the pressure near the seabed in wellbores and pipelines often surpasses this threshold, facilitating hydrate formation. Hydrate formation and accumulation may abruptly reduce the effective flow area in wellbores and pipelines, increasing pressure and flow velocity and thereby threatening the safety of production operations. In more severe cases, complete blockage of the wellbore or pipeline may occur, potentially resulting in catastrophic incidents such as blowouts [27]. Therefore, predicting and evaluating hydrate formation in wellbores and pipelines during deepwater oil and gas development are of great relevance to engineering significance and research value.

To date, numerous researchers have investigated behavior of multiphase flow in wellbore during deepwater oil and gas development and have achieved notable progress. Yang et al. [28] numerically investigated the thermodynamic and multiphase flow behavior in wellbore during gas invasion in downhole dual-gradient drilling (DDGD) with oil-based drilling fluid. It was found that drilling conditions, transient interface mass transfer and wellbore temperature can all significantly influence behavior of multiphase flow in wellbore. Yu et al. [29] investigated the effects of gas influx and lost circulation on the temperature distribution and gas flow within the wellbore, and analyzed the evolution characteristics of gas influx and lost circulation under varying operation parameters. The investigation results reveal that gas expansion following a gas influx occurs above 200 meters, while lost circulation leads to significant decreases in wellhead temperature, bottom-hole temperature, and bottom-hole pressure. Chen et al. [3] conducted transient simulations of wellbore temperature and pressure profiles during deepwater gas well cleaning operation, and subsequently developed a hydrate risk prediction model to evaluate the potential for hydrate formation. The research findings demonstrate that measures such as improving liquid-to-gas ratios, and the use of inhibitors can effectively mitigate the risk of hydrate formation in wellbore. Fu et al. [30] investigated the evolution of wellbore parameters, such as temperature and pressure, during deepwater drilling operation, and analyzing the multiphase flow behavior and phase transitions of gas hydrates in wellbore. The findings indicate that a higher circulation rate moves the wellbore section of hydrate formation upward from the seabed, and the casing shut-in pressure fails to capture information about gas kick resulting from hydrate formation. While these studies are valuable for ensuring operation safety during deepwater oil and gas development, they still exhibit certain shortcomings that require further investigation. The main limitations include:

1. Most existing studies are conducted on drilling operations and are based on accidents such as gas invasion and well kick.
2. The formation of gas hydrates in wellbore and the associated risks have often been overlooked in previous investigations.
3. The scope of existing research is largely confined to the internal environment of the wellbore. In other words, previous studies have primarily focused on well control and the safety of drilling operations.

This study aims to provide flow assurance strategies and technical references to support the future development of deepwater turbidite reservoirs. In this paper, the main contributions this are outlined as follows.

- To address the issue of hydrate deposition in subsea pipelines, numerical simulations were conducted to investigate the temperature and pressure variations within both the wellbore and the subsea pipelines. Meanwhile, potential locations within the wellbore and pipeline where gas hydrates may form and accumulate were identified, facilitating the implementation of targeted mitigation strategies during operation design.
- Based on the characteristics of subsea transportation system, the formation mechanisms and stability conditions of natural gas hydrates are reviewed. Meanwhile, targeted engineering strategies were proposed to mitigate the risk

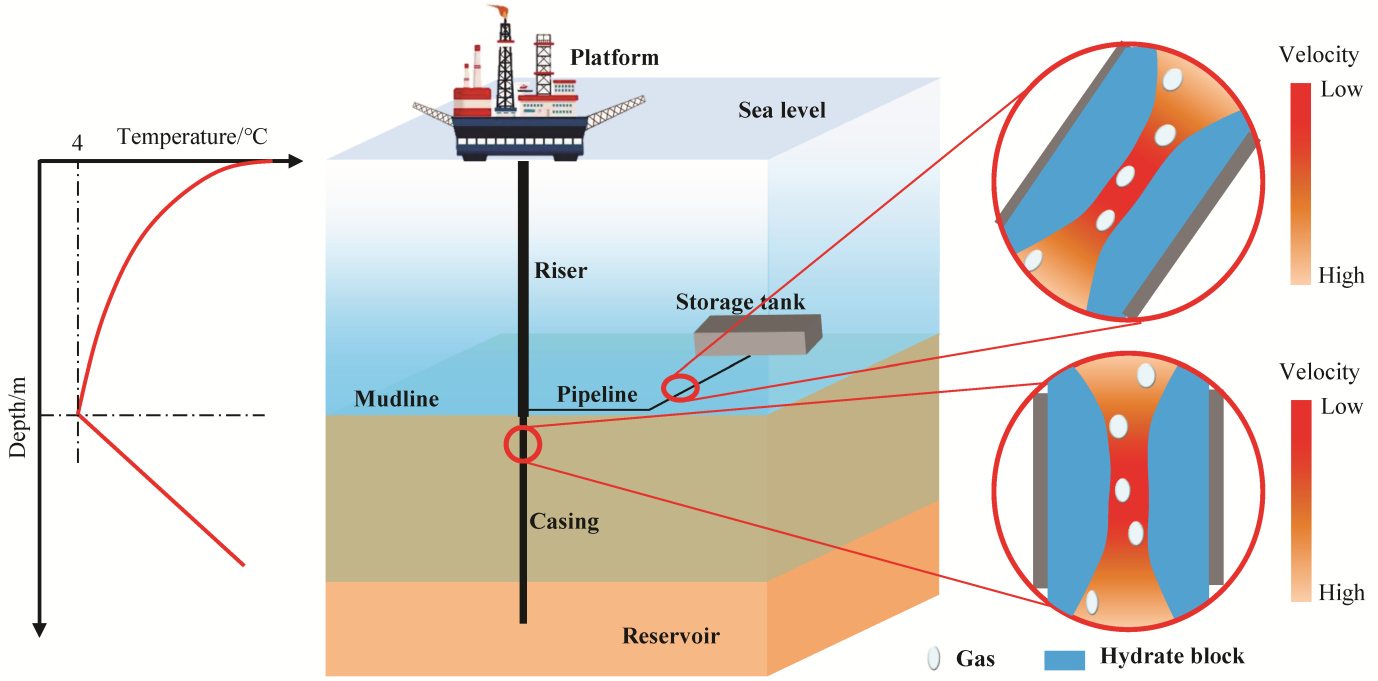

Figure 1. Schematic of hydrate formation and accumulation in wellbores and pipelines.

of pipeline blockage by hydrate formation and accumulation, and the feasibility was also evaluated.

Motivated by the above presented contributions and insights, the structure of this study is summarized as follows. In Section 2, a coupled mathematical model was established to simulate the two-phase flow and hydrate formation within the wellbore and subsea pipeline, and its applicability was validated through comparative analysis. In Section 3, the risk of hydrate formation in the investigation system was evaluated. In Section 4, the effects of methanol, one inhibitor, on the risk of hydrate formation were experimentally investigated, and preliminary design optimization was proposed.

2 Mathematical Model

Owing to the structural discrepancies between the wellbore and pipeline in the modeled system, separate mass, momentum and energy conservation equations must be developed for the fluids in both. To facilitate the modeling and investigation, the fluids in the subsea pipeline and wellbore were selected as the research subjects, and the micro-elements were illustrated in Figure 2. The following assumptions were made to simply the mathematical model. (1) The fluid flow is simplified to the axial direction within the wellbore and subsea pipeline by neglecting the radial velocity component. Consequently, temperature and pressure variations occur primarily along the axial (length) dimension. (2) The mathematical model's scope is restricted to the simulation of hydrate formation from gas and water phases, neglecting the reverse processes of dissociation. (3) Latent heat release during hydrate formation is neglected in the energy balance calculation, assuming the thermal contributions from phase change within the system are negligible. (4) The physical properties of the gas, liquid, and solid phases are assumed to be uniform across each investigation element. (5) The external temperature field (formation or seawater) of the wellbore or pipeline remains constant, and heat transfer is treated as purely conductive, neglecting the effect of heat radiation. (6) Methane constitutes the entire gas composition, with all other non-methane gases being neglected from the analysis.

2.1 Mass conservation equation

As observed in Figure 2, the micro-element in the subsea pipeline or wellbore is modeled as a cylinder with radius r and length dx. Although the model radius varies between the wellbore and pipeline, the mass conservation equation retains the same general form. Therefore, a unified expression for the mass conservation equation applicable to both the wellbore and pipeline is presented herein.

Within this element, a three-phase flow exists–comprising a liquid phase (water, denoted as l), a gas phase (natural gas, denoted as g) and a

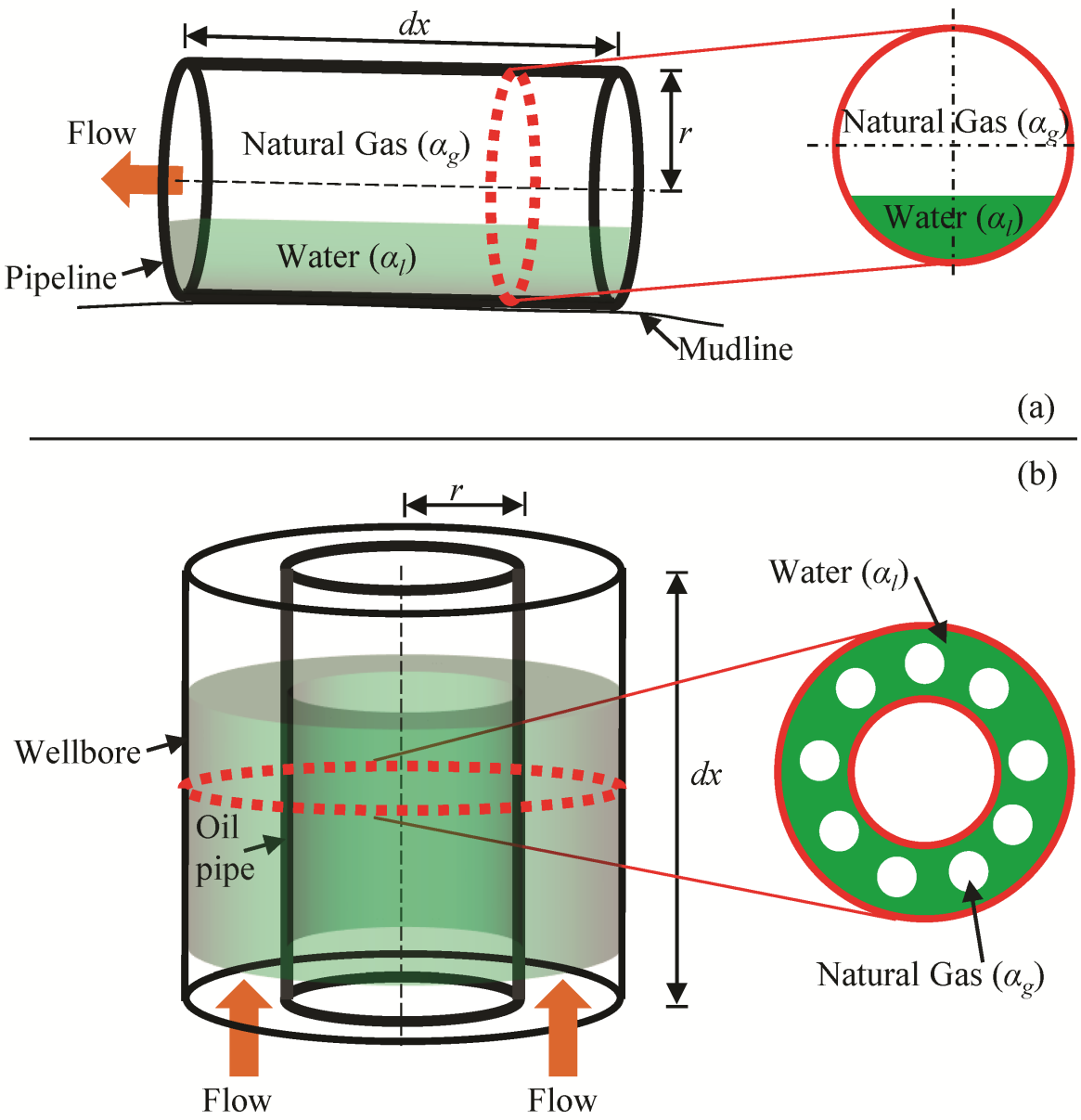

Figure 2. Schematic diagram of fluid micro-elements in (a) subsea pipelines and (b) wellbores during gas production stage.

solid phase (gas hydrate, donated as h)–with volume fractions represented by α_l, α_g, and α_h, respectively. In addition, natural gas, water, and hydrate flow through the pipeline or wellbore at velocities v_g and v_l, and v_h, respectively. Based on mathematical derivation, the mass conservation equations for the gas, liquid, and hydrate phases within the subsea pipeline or wellbore are obtained, and presented in Equation 1 [31, 32].

$$\begin{cases} \text{Gas Hydrte:} \frac{\partial(Aa_h\rho_h)}{\partial t} + \nabla \cdot (Aa_h\rho_h\nu_h) = m_h \\ \text{Water phase:} \frac{\partial(Aa_l\rho_l)}{\partial t} + \nabla \cdot (Aa_l\rho_l\nu_l) = S_l \\ \text{Gas phase :} \frac{\partial(Aa_g\rho_g)}{\partial t} + \nabla \cdot (Aa_g\rho_g\nu_g) = S_g \end{cases} \tag{1}$$

where ρ is the density of gas, liquid, and hydrate phases, t is time, A is the cross-sectional area of a pipeline or wellbore, S_g and S_l are the consumption rate of natural gas and water for hydrate formation respectively. Since this study only considered the formation of gas hydrates (rather than its dissociation), both S_l and S_g are negative throughout the simulation, and contingent on the phase change of gas hydrates. The expressions for determining the parameters S_l and S_g due to hydrate formation are given by:

$$\begin{cases} S_l = -\frac{5.75M_{\mathrm{H2O}}}{M_{\mathrm{CH4}}+5.75M_{\mathrm{H2O}}} m_h \\ m_h = k_h A_s \left(p - p_{eq}\right) a_l a_g \\ S_g = -\frac{M_{\mathrm{CH4}}}{M_{\mathrm{CH4}}+5.75M_{\mathrm{H2O}}} m_h \end{cases} \tag{2}$$

where M_{H2O}, M_{CH4} are molecular weight of water and methane respectively, k_h is the reaction rate constant, A_s represents the gas–liquid interfacial area, p is the pressure. Notably, p_{eq} is the phase equilibrium pressure of methane hydrate, which should be determined by the following equation [28]:

$$P_{eq} = 9 \times 10^{-14} e^{0.1136T} \tag{3}$$

where T is the temperature in pipeline, and e is the natural constant.

2.2 Momentum conservation equation

Through the momentum conservation equation, the effects of pressure, gravity, and viscosity on the gas and liquid phases are quantified, enabling the prediction of the velocity fields and flow characteristics. As with the mass conservation equation, the form of the momentum conservation equation remains consistent for fluids in both the wellbore and the pipeline [29, 33]. Essentially, the momentum conservation theorem states that the derivative of an object's momentum with respect to time is equal to the net external force acting on it, and can be expressed as:

$$\frac{d}{dt}(m\nu) = \sum F \tag{4}$$

Through mathematical derivation, the momentum conservation equations for the fluid inside the pipeline and wellbore are obtained as follows:

$$\begin{aligned} &\frac{\partial}{\partial t}\left(\sum_{i=g,w,h}(a_i\rho_i\nu_i)\right) + \nabla\cdot\left(\sum_{i=g,w,h}\left(a_i\rho_i\nu_i^2\right)\right) \\ &+ g\cos\beta\left(\sum_{i=g,w,h}(a_i\rho_i)\right) + \nabla\cdot(p) + \nabla\cdot(F_r) = 0 \end{aligned} \tag{5}$$

where β is the angle between the wellbore or pipeline and the direction of gravity. F_r is the frictional pressure drop, which can be determined by

$$\begin{cases} F_r = \frac{2f\rho_m\nu_m}{d} \\ f = \frac{0.0655+1.8598\varepsilon}{R_e^{0.25}(1-a_g)^x} \end{cases} \tag{6}$$

where ε is the roughness, Re is the Reynolds number, d is the diameter. ρ_m is the density of the mixed fluid, which can be determined by $\rho_m = \rho_g\alpha_g + \rho_l\alpha_l$. In addition, v_m is the flow velocity of mixed fluid, which was determined by $v_m = v_g\alpha_g + v_l\alpha_l$. x is the experimental coefficient, which is 0.25 and 8.75 for bubbly flow and slug flow, respectively.

2.3 Energy conservation equation

Accurate prediction of the temperature within the pipeline is essential for evaluating the risk of hydrate formation, highlighting the necessity of deriving the energy conservation equation [34, 35]. Assuming negligible latent heat during hydrate formation and no other heat sources, the energy conservation equation of the fluid in the submarine pipeline was proposed. In this section, the mathematical derivation is carried out in detail. Through mathematical derivation, the energy conservation equation governing the unsteady gas–liquid flow in the wellbore annulus is obtained as follows [36]:

$$\frac{\partial}{\partial t}(\rho_m c_m T_a) - \nabla\cdot(c_m T_a \nu_m) = 2\left(\frac{1}{A'}(T_s - T_a)\right) \tag{7}$$

where T_a is the fluid temperature inside the annulus, T_s is the sediment temperature around wellbore. c_m is the specific heat of the mixed fluid in pipeline, which can be determined by $c_m = c_g\alpha_g + c_l\alpha_l$.

Similarly, the energy conservation equation governing the fluid inside submarine pipelines can be expressed as:

$$\frac{\partial}{\partial t}(\rho_m c_m T_p) - \nabla\cdot(c_m T_p \nu_m) = 2\left(\frac{1}{B'}(T_w - T_p)\right) \tag{8}$$

where T_p is the fluid temperature inside the pipeline, T_w is the water temperature at the seabed.

The parameter A' in Equation 7, as well as parameter B', can be calculated by the following equation.

$$\begin{cases} A' = \frac{1}{2\pi}\left(\frac{k_e + r_{co}U_a T_D}{r_{co}U_a k_e}\right) \\ B' = \frac{1}{2\pi r_{pi}U_t} \end{cases} \tag{9}$$

where k_e is the thermal conductivity of the sediment around wellbore, r_{co} is the outer diameter of annulus, r_{pi} is the inner diameter of submarine pipelines, T_D is the transient heat transfer function, U_a is the total thermal conductivity of the casing and the sediment, U_t is the total thermal conductivity of the pipeline.

Based on the above derivations, the spatial distribution of temperature and pressure along the pipeline and wellbore can be obtained, providing basic for determining potential hydrate formation regions in subsea pipeline and wellbore.

2.4 Model verification

It is essential to verify the applicability of this mathematical model before applying it to numerical prediction of hydrate formation in production and transport system of deepwater oil and gas. In this study, the applicability of the model was validated by comparing its predicted temperature and pressure values with experimental data. The experimental system employed to verify the mathematical model's applicability is shown in Figure 3. As observed in Figure 3(a), the experimental device is a vertical wellbore model, with outer and inner diameters of 20 cm and 12 cm, respectively. The wellbore model is made of acrylic plastic, with a wall thickness of 0.5 cm and a maximum pressure tolerance of 12 MPa. Moreover, the 5-meter-long wellbore was placed in a cold storage during the experiment to replicate the low-temperature environment near the seabed. During the experiment, a mixture of natural gas and water was injected into the annulus at a controlled rate through the lower section of the wellbore, allowing it to rise freely. In order to restore deepwater conditions, a back pressure valve was configured at the top end of the annulus. Thus, by regulating the back pressure in the annulus, hydrostatic conditions equivalent to those at depths of several kilometers can be effectively simulated. As an example, 10 MPa of back pressure is roughly equivalent to the pressure exerted by a 1,000 m water column under standard seawater density conditions. Moreover, from Figure 3(a), it can be observed that three sensor-equipped measuring sections are positioned at the upper, central, and lower portions of the wellbore to monitor temperature and pressure. For clarity, the three measurement sections are designated as Sections 1, 2, and 3 from the bottom upward.

In addition, the experimental apparatus includes several supporting subsystems, such as a water circulation system, gas tank, and a pressurization device. Real-time data acquisition was implemented during the experiment, with a sampling interval of 2.0 minutes. For model verification, the experiment was conducted under the following primary conditions: gas-liquid mixture injection rate of 0.5 m^3/min, injected fluid temperature of 10°C, a back pressure

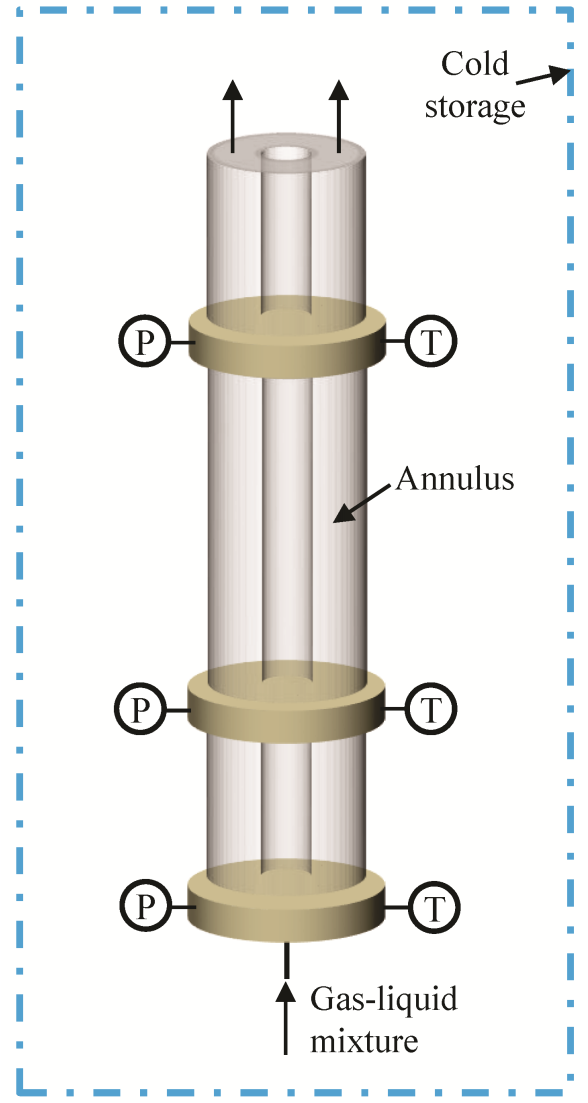

(a)

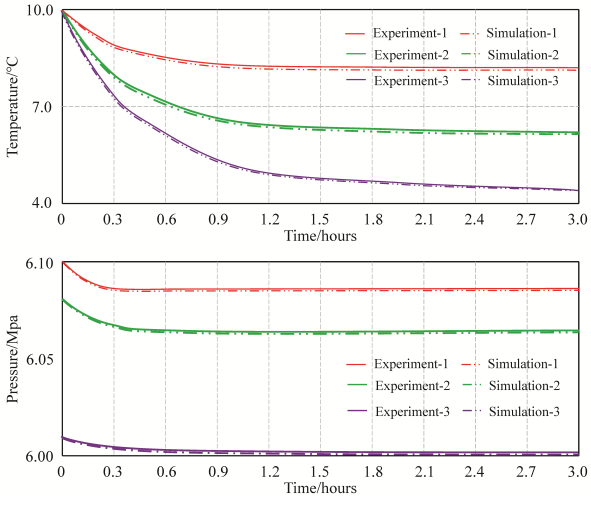

(b)

Figure 3. (a) Experimental system employed to verify the mathematical model's applicability and (b) the verification result.

of 6.0 MPa, and a cold storage temperature of 4.0°C. Besides, the injected gas is methane with a purity of 99.9%, and the pressure in the pipeline is determined by factors such as gas injection flow rate and flow pattern. Of course, the circular tube in the experimental system is positioned vertically. Based on the above experimental conditions, the simulation results were compared with the experimental data, as illustrated in Figure 3(b). It can be observed from Figure 3(b) that the simulation outcomes are generally consistent with the experimental results, as the differences between the dashed and solid curves are negligible. Taking the temperature and pressure measurements at 3 hours as an example, the root-mean-square errors (RMSEs) for temperature and pressure are 0.061 °C and 0.0033 MPa, respectively. Similarly, the RMSE values at other time points are also very small, indicating a high level of agreement between the simulated and measured data. The findings suggest that the developed model can serve as a reliable tool for predicting temperature and pressure profiles, as well as hydrate formation behavior, in wellbores and pipelines in the context of deepwater oil and gas development. Despite the overall agreement, a subtle difference persists between the simulation and experimental outcomes. The primary reason for this deviation is that, during the experiment, the flow pattern temporarily shifted to intermittent bubbly flow, while the simulation consistently considered a slug flow pattern.

3 Prediction of hydrate formation in transport and production system

3.1 Modeling of submarine pipeline system

Engineering data collected from an oilfield in the northern South China Sea indicate that it adopts a development model combining FPSO (Floating Production Storage and Offloading) and subsea wellheads [37]. Furthermore, the drilling vessel was used to support the drilling operations. The oil and gas extracted from the subsea wellhead are transported to the FPSO for storage via manifolds, flexible risers, and other facilities. In this study, the term "submarine pipeline" specifically refers to the pipeline section between the subsea wellhead and the FPSO. In this study, the subsea pipeline system is assumed to consist of four main components: jumper pipe, production flowline, risers, and flexible riser. As can be seen in Figure 4, the subsea wellhead is defined as the flow inlet, while the FPSO is defined as the pressure outlet. The inlet flow corresponds to the production rate of oil and gas from the wellhead, whereas the pressure outlet corresponds to the pressure in FPSO. To better illustrate the structure of the four components, Figure 5 presents the three-dimensional schematic diagram.

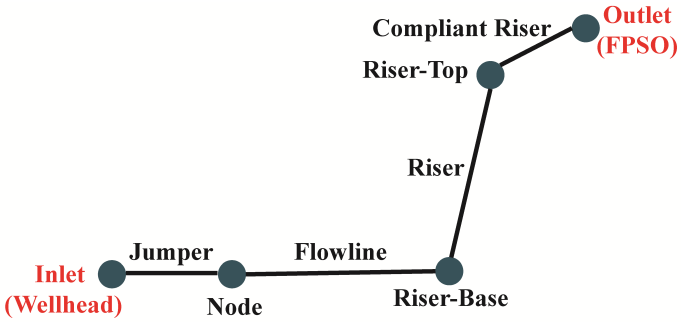

Figure 4. The submarine pipeline system developed in this study.

Jumper pipe is a key component of subsea production systems in deepwater oil and gas development. It plays a critical role in connection and flow transfer, ensuring the efficient and safe transport of oil and gas from the wellhead to processing facilities (such as FPSO). As shown in Figure 5(a), four layers are identified from the inside to the outside of the jumper pipe: steel inner pipe, FBE+PP adhesive layer, PP syntactic layer, and PP solid layer. Among them, the solid polypropylene (i.e., the PP Solid) layer primarily serves to provide mechanical protection and polypropylene syntactic (i.e., PP Syntactic) layer is typically used for thermal insulation and buoyancy control. However, the adhesive layer of epoxy powder (FBE) and polypropylene (PP) is used to enhance the adhesion between the inner pipe and the outer insulation layer.

As observed in Figure 5(b), the flowline comprises six layers from the inside out: the inner pipe, epoxy (FBE) layer, insulation layer (aerogel), air gap layer, outer pipe, and 3LPE layer. Specifically, the 3LPE layer and outer pipe are designed to provide mechanical protection and structural support, whereas the air gap and aerogel insulation layers are responsible for minimizing heat loss and maintaining thermal stability within the pipeline. In addition, the function of epoxy powder coating (FBE) layer is to enhance the corrosion resistance of pipelines. A comparison between Figure 5(c) and Figure 5(a) reveals that the riser contains an additional mid-layer of PP Solid material, which contributes to enhanced thermal insulation compared to the jumper pipe.

Furthermore, the flexible working environment necessitates a correspondingly intricate structural design for compliant risers. As presented in

Table 1. Basic parameters of the jumper pipe, flowline, riser and flexible riser.

Components	Layer	Thickness/mm	Conductivity/(W/m/k)	Density/(kg/m^3)	Specific heat/(J/kg/K)
Jumper pipe	Pipe	14.3	45	7850	480
	FBE+PP Adhesive	0.5	0.22	900	2000
	PP Syntactic	70	0.18	685	2000
	PP Solid	4	0.22	900	2000
Flowline	Pipe	25.4	45	7850	450
	Epoxy(FBE)	0.2	0.3	1440	2000
	Insulation layer	18.4	0.013	90	1050
	Air Gap	22.5	0.14	1.2	1000
	Outer Pipe layer	31.8	45	7850	450
	3LPE layer	2.4	0.22	900	2000
Riser	Pipe	25.4	45	7850	480
	FBE+PP Adhesive	0.45	0.22	900	2000
	PP Solid	7	0.22	900	2000
	PP Syntactic	68.5	0.16	685	2000
	PP Solid	4	0.22	900	2000
Flexible riser	Pipe	8	1161	4850	502
	Gammaflex layer	7	0.2	1700	1380
	Zeta layer	10	0.94	7100	502
	Armour layer	10	0.94	7100	502
	TPFLEX layer	21	0.2	940	1805
	Insulation layer	10.2	0.15	722	1900
	TPFLEX layer	21	0.2	940	1805

Figure 5(d), the flexible riser is composed of, from the inside out, a pipe, Gammaflex layer, Zeta layer, Armor layer, TPFLEX middle layer, Insulation layer, and TPFLEX outer protective layer. This multilayer design integrates the strength of steel with the flexibility and heat insulation of polymers, meeting the complex demands of deep-sea flexible riser transport. For simulation purposes, the characteristic parameters of the four pipeline types in the subsea pipeline system are summarized in Table 1.

3.2 Modeling of wellbore structure and gas composition

The structural configuration of the wellbore directly influences the distribution of temperature and pressure within it. In this study, a development well in the South China Sea gas reservoir, located in the Baiyun Sag of the Pearl River Mouth Basin, is selected as a case study. The corresponding wellbore structure is shown in Figure 6.

As can be seen in Figure 6, this is a vertical well for gas production from deepwater gas reservoir, and the total well depth is 1510 m, and water depth is 510 m. Besides, the seabed temperature at the well site is 4°C, and the geothermal gradient is estimated to be 2.0°C/100 m. From Figure 6, it can also be seen that the wellbore consists of three sections: the conductor, surface casing, and production casing. The 30-inch (762mm) conductor penetrates 80 m beneath the seabed. However, the setting depth for the $13\frac{3}{8}$-inch surface casing and the $9\frac{5}{8}$-inch production casing are 618.5 m and 3368.5 m, respectively. Meanwhile, a 5-inch sucker rod runs along the wellbore axis throughout its entire length.

The composition of the extracted fluid is also an important factor influencing the temperature and pressure distributions in wellbore or pipeline, as well as the phase equilibrium conditions of gas hydrate. In this study, the extracted fluid from the gas reservoir consisted primarily of natural gas, with a low water content of 15%. The composition of the fluid produced from the gas well, as well as the phase equilibrium curve, is shown in Figure 7. From Figure 7(a), it is evident that methane is the predominant component of the produced gas, accounting for approximately 90.5%, followed by ethane at about 7.5%, and carbon dioxide at only 2.0%. The gas composition suggests that the reservoir is a CO_2-poor gas reservoir.

According to the composition of gas shown in Figure 7(a), the phase equilibrium curve was obtained from calculations performed with the CSMHYD program [38], and the results was present in Figure 7(b). As can be seen in Figure 7(b), the presence of CO_2 and ethane enlarges the hydrate stability zone (i.e., the upper-left

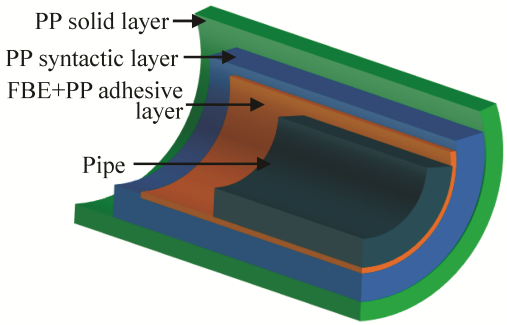

(a) Jumper pipe

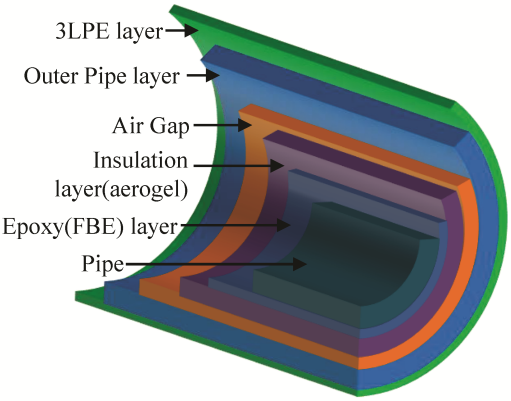

(b) Flowline

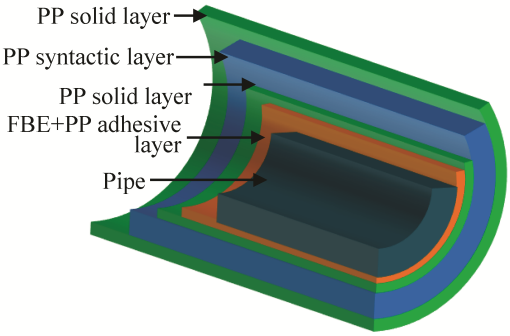

(c) Riser

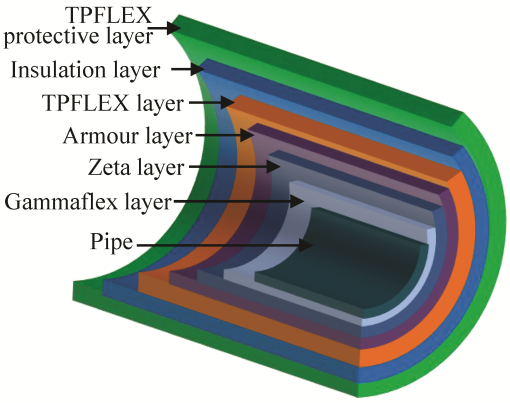

(d) Flexible riser

Figure 5. Cross-sectional schematic of the four main components of the subsea pipeline system.

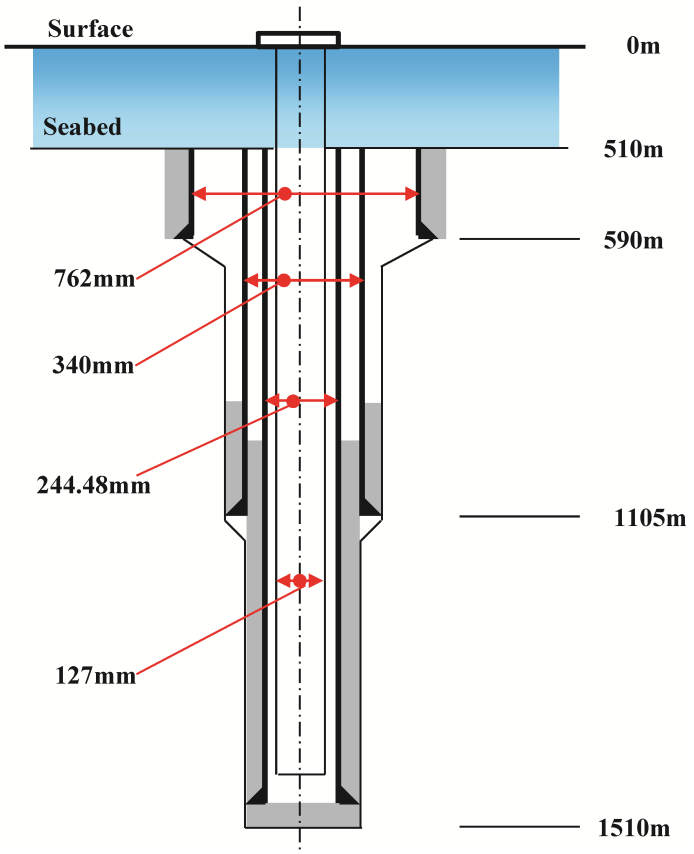

Figure 6. Wellbore structure of the study case.

area), indicating a higher risk of hydrate formation to some extent. Meanwhile, the initial production rate of the research wellbore is 0.5×10^6 m^3/day. In the subsequent analysis, it is assumed that parameters, including gas production rate and water content, follow the trends depicted in Figure 8 throughout the entire production process. From Figure 8, it can be seen that the production rate exhibits a gradual decline, accompanied by a progressive increase in water content during the development process. It is noteworthy that, despite variations in gas production rate and water content during the gas production process, the composition of the gas phase remains largely unchanged.

3.3 Simulation results and discussion

Based on the above theoretical framework, simulations of the temperature and pressure distributions within the wellbore and pipeline were carried out, along with a risk assessment of hydrate formation. In this section, the risk assessment results of the hydrate formation conducted for different production cycles were presented.

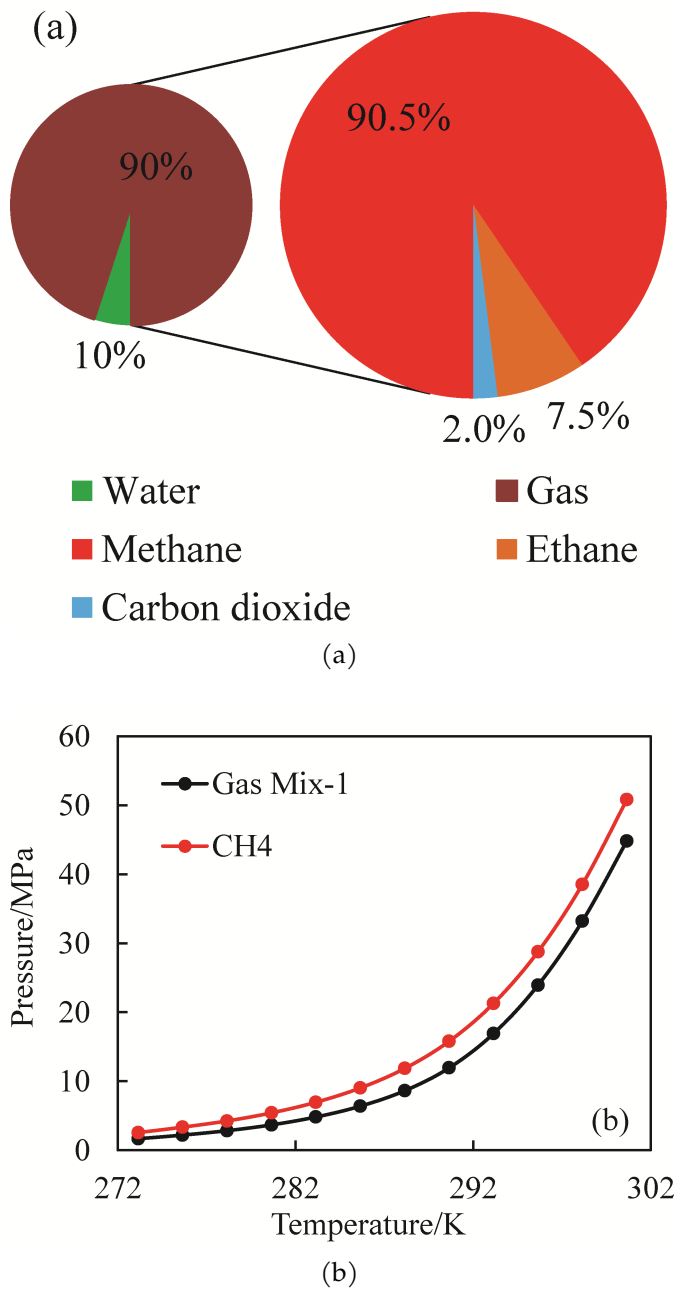

Figure 7. (a) Initial composition of produced fluid in gas wells and (b) the phase equilibrium conditions.

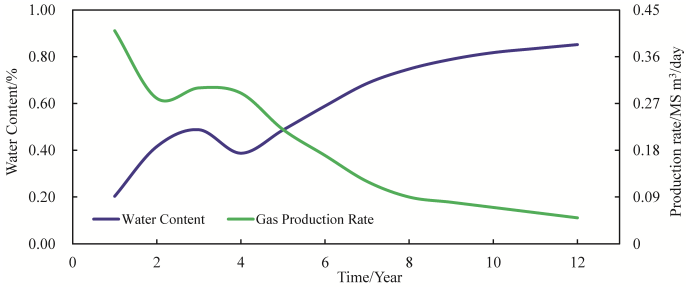

Figure 8. Evolution of production parameters throughout the production cycle.

3.3.1 *Risk prediction of hydrate formation in wellbore*

The risk assessment of hydrate formation in wellbore or pipeline requires a clear specification of the criterion or method used for its determination. As the first step in this criterion or method, it is necessary to numerically determine the temperature profile along the pipeline or wellbore. Thereafter, the phase equilibrium pressure profile is derived from the temperature data, combined with the hydrate phase equilibrium relationship shown in Figure 7(b). Of course, the equilibrium pressure depends on the specific composition of the gas functioning as the guest molecule. Ultimately, the risk of hydrate formation is determined by assessing the deviation between the actual pressure at any location in the wellbore or pipeline and the corresponding phase equilibrium pressure. The risk of hydrate formation arises when the actual pressure exceeds the corresponding phase equilibrium pressure, while no such risk occurs if the actual pressure remains below the equilibrium value. This methodology enables the identification of wellbore and pipeline sections at risk of hydrate formation, thereby providing guidance for targeted prevention and control measures.

In the early stages, limited heat transfer occurs between the wellbore fluid and the surrounding sediments, with the wellbore fluid temperature primarily governed by the reservoir fluid temperature. That is, axial heat transfer is significantly stronger than radial heat transfer. However, the fluid inside the wellbore always maintains a higher temperature compared to the surrounding sediments throughout the development operation. Heat transfer between the elevated-temperature wellbore fluid and the sediment around wellbore is inevitable. As the gas reservoir is developed over time, the temperature of the extracted fluid in the later stages of production operation becomes gradually more dependent on the surrounding sediment's thermal influence. Figure 9 illustrates the profiles of temperature, pressure, and phase equilibrium pressure within the wellbore at various stages of production operation. According to the results presented in Figure 9, the fluid temperature in wellbore increases initially and then decreases over the course of the gas reservoir production simulation. Taking the investigation node of wellhead as an example, the temperatures obtained in the 1^{st}, 4^{th}, 8^{th}, and 12^{th} years of development operation were 17.55°C, 17.88°C, 16.23°C, and 15.74°C, respectively. Moreover, the temperature profile of the fluid within wellbore becomes relatively stable after about 10 years of continuous development operations. In line with

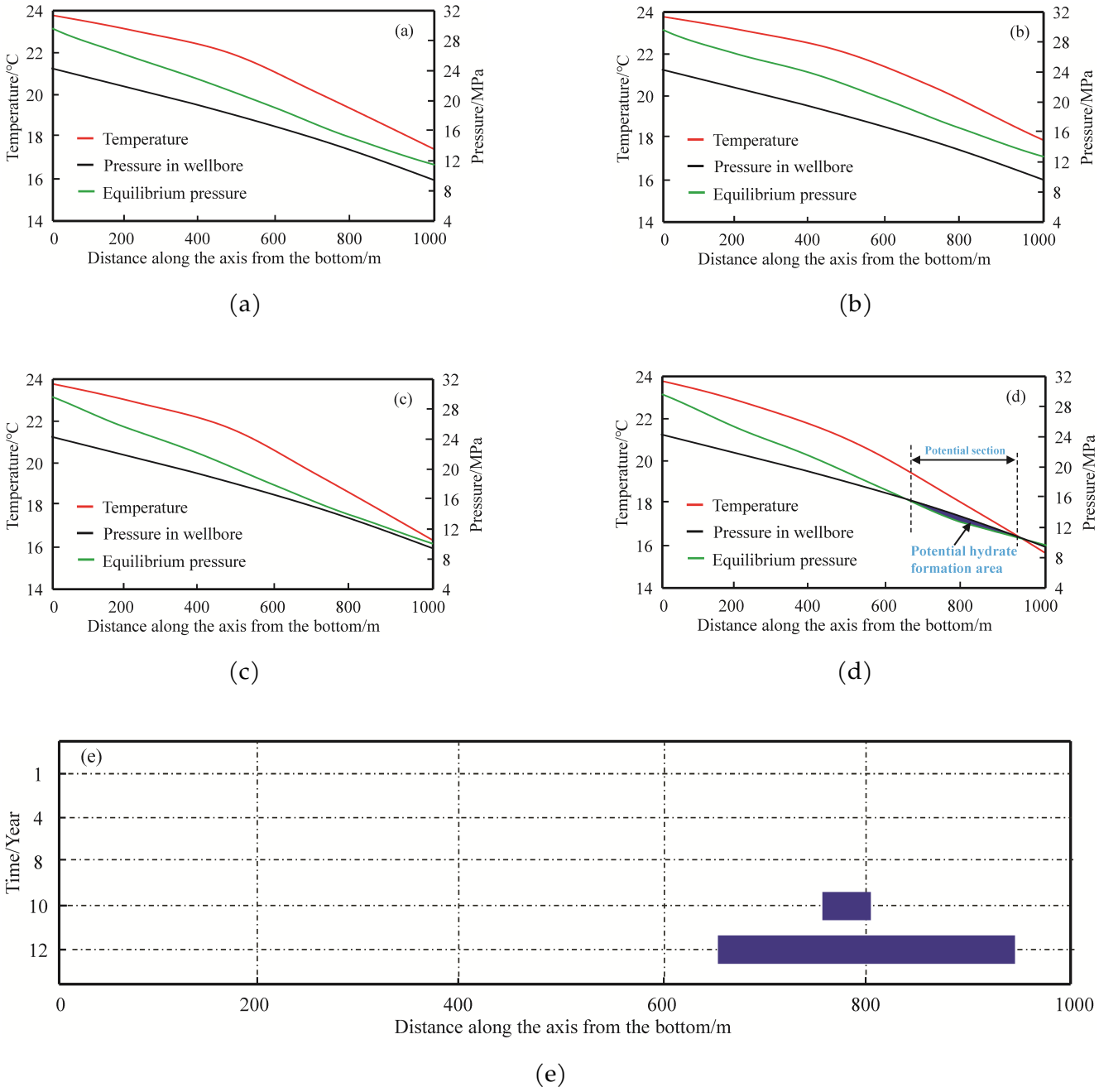

Figure 9. Evolution curves of temperature and pressure profiles inside the wellbore. (a) 1 year; (b) 4 years; (c) 8 years; (d) 12 years; (e) Potential risk section.

this, the equilibrium pressure profile exhibits a trend of initial increase followed by a subsequent decrease. However, the in-situ pressure profile exhibits only minor variations over the entire development process. According to Figure 9(a), the equilibrium pressure is higher than the actual pressure during the early stage of development operation. With the variation in equilibrium pressure, the equilibrium pressure profile may intersect the actual pressure profile at specific locations along the wellbore during the development process.

It can be seen from Figure 9 that, over the first eight years of development operation, neither of the two pressure profile curves intersected (see Figures 9(a-d)). This means that the wellbore remains free from the risk of hydrate formation throughout this timeframe. After approximately 10 years of gas production from the turbidite reservoir, an intersection between the equilibrium and actual pressure profiles first emerged, marking the initiation of hydrate formation risk. At this moment, a potential risk of hydrate formation exists within the 49 m wellbore interval extending from 754 to 803 m above the well bottom (see Figure 9(e)). Obviously, the changes in

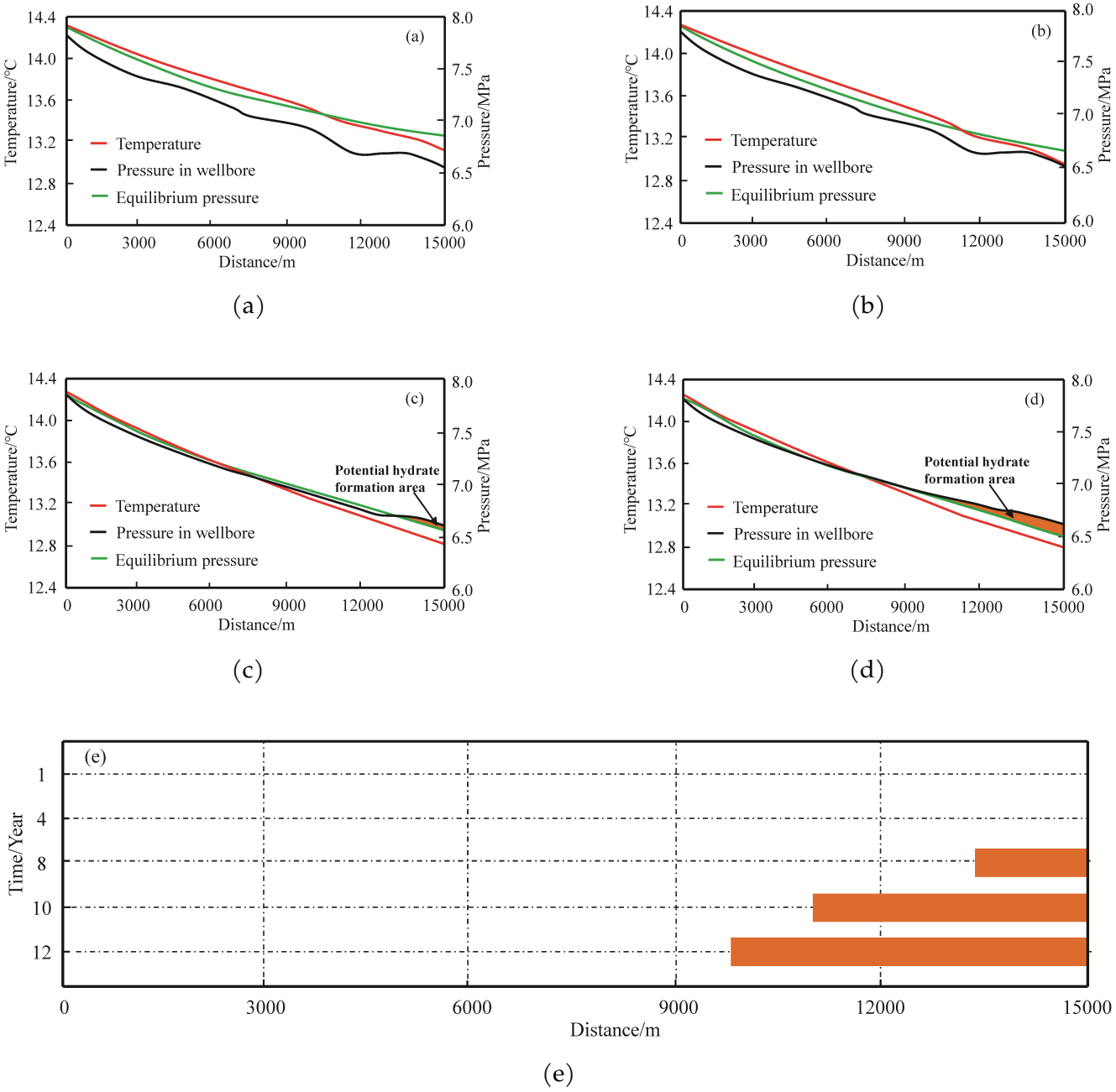

Figure 10. Risk evolution results of hydrate formation in submarine flowline. (a) 1 year; (b) 4 years; (c) 8 years; (d) 12 years; (e) Potential risk section.

actual pressure profile along the wellbore are minimal throughout the entire production process. This 49 m risk section in the wellbore after 10 years arises mainly from the decreasing equilibrium pressure, which caused the local pressure to exceed the hydrate phase equilibrium boundary. With relatively stable low temperatures, this pressure dominance facilitates hydrate nucleation and particle agglomeration near the casing shoe. In subsequent stages of gas production, the potential interval with the risk of hydrate formation progressively extends, and the risk of wellbore blockage by hydrates further increases. At the end of simulation, the wellbore section at risk of hydrate formation extends to a 265 m interval, spanning from 663 m to 928 m, measured from the well bottom. It is necessary to implement measures to mitigate hydrate formation and blockage within the wellbore, thereby ensuring the safe and efficient development of gas reservoirs. It should be noted that these measures and their corresponding effects will be discussed in Section 4.

3.3.2 Risk prediction of hydrate formation in flowline pipe

The fluid temperature in subsea pipelines is readily reduced by the surrounding seawater, promoting hydrate formation within the pipeline, which may

obstruct the flow of produced fluids to the FPSO. In light of this, the likelihood of hydrate formation in subsea pipelines merits detailed investigation.

Figure 10 presents the risk assessment results of hydrate formation for long-distance submarine flowline. We can see from Figure 10 that, the fluid temperature decreases gradually along the flowline, and all the temperature profiles are smooth regardless of the irregular seabed topography. This result suggests that the fluid temperature inside the flowline is largely independent of variations in seabed topography. However, the pressure profile along the flowline exhibits noticeable fluctuations, with a relatively mild gradient observed between 11,900 m and 13,800 m (see Figures 10(a–d)). This phenomenon can be attributed to the relatively flat seabed topography supporting this section of the flowline. In addition, across the 15.0 km flowline, the fluid temperature drop increases from 1.1 °C to 1.5 °C throughout the simulation. The phenomenon arises because the seawater temperature at seabed in deep-sea areas is generally maintained at approximately 3–4 °C, causing unavoidable heat exchange between the "hot" flowline fluids and the ambient seawater. In the later stage, the combined effects of declining production rate and increasing water content intensify the heat exchange between the high-temperature fluid and the surrounding environment, while simultaneously reducing the axial heat supply. This synergistic effect ultimately results in a more pronounced temperature decline along the pipeline. Accompanying this, the equilibrium pressure progressively decreases as the gas production project advances. In contrast, the pressure within long-distance flowline exhibits a slight increase. There exist specific research conditions under which the equilibrium pressure intersects with the actual pressure, resulting in hydrate formation that poses the risk of pipeline blockage.

According to Figure 10, after 6.4 years of the gas production, certain flowline section displays gas phase pressure surpassing the phase equilibrium pressure, and it is situated at its end. From this moment, the intersection region between the two pressures gradually expands, and the flowline section susceptible to hydrate formation correspondingly increases in length. After 8.0, 10.0, and 12.0 years of gas production, the flowline sections at risk of hydrate formation extend to 2500 m, 4200 m, and 4850 m, respectively. The formation and potential blockage of gas hydrates in long-distance flowline can severely compromise the safety of storage, transportation, and temporary containment of the produced fluids.

3.3.3 Risk prediction of hydrate formation in riser

The riser, entirely submerged in seawater, connects the subsea flowline to the platform at both ends. Along the riser, the fluid temperature increases progressively in the flow direction (see Figure 1), whereas the pressure exhibits a gradual decline. Theoretically, the risk of hydrate formation decreases as the flow approaches the riser's endpoint. Nevertheless, hydrates may still form in the riser near the seabed throughout the duration of gas production. Therefore, it is necessary to analyze the distributions of temperature, pressure, and phase equilibrium pressure in the riser to identify and quantify the sections with potential hydrate risks. The evaluation results are shown in Figure 11.

According to Figure 11, the temperature and pressure of the fluid within the riser gradually decrease along the flow direction at any development moment. In this case, the phase equilibrium pressure determined by fluid temperature and the actual pressure in the riser exhibit similar trends. Fortunately, the variation in actual fluid pressure occurs at a faster rate than that of the phase equilibrium pressure induced by fluid temperature. As a result, the riser section at risk of hydrate formation is primarily located in proximity to the seabed. As anticipated, a 9.8 m section at risk of hydrate formation emerged in the riser near the seabed by the eighth year of the gas production project (see Figures 11(c, e)). Following this, the actual pressure in the riser section close to the seabed experiences a slight increase. In contrast, the phase equilibrium pressure within the same riser section steadily diminishes. The result is that the hydrate-prone riser section near the seabed continues to extend after 8 years. By the 10th year, this riser section length reached 21.2 m, further extending to 38.4 m in the 12th year. Based on the results shown in Figure 11(e), it can be inferred that with the continued extraction of the gas reservoir, the length of the riser section prone to hydrate formation may continue to increase slightly.

By comparing the results presented in the preceding three sections, it is evident that long-distance flowline laid on the seabed exhibit the highest probability of hydrate formation and blockage risk. Although relatively low, the risk of hydrate formation in the riser still exists. Therefore, it is essential to investigate appropriate engineering strategies to mitigate hydrate formation and prevent blockages in production and gathering systems.

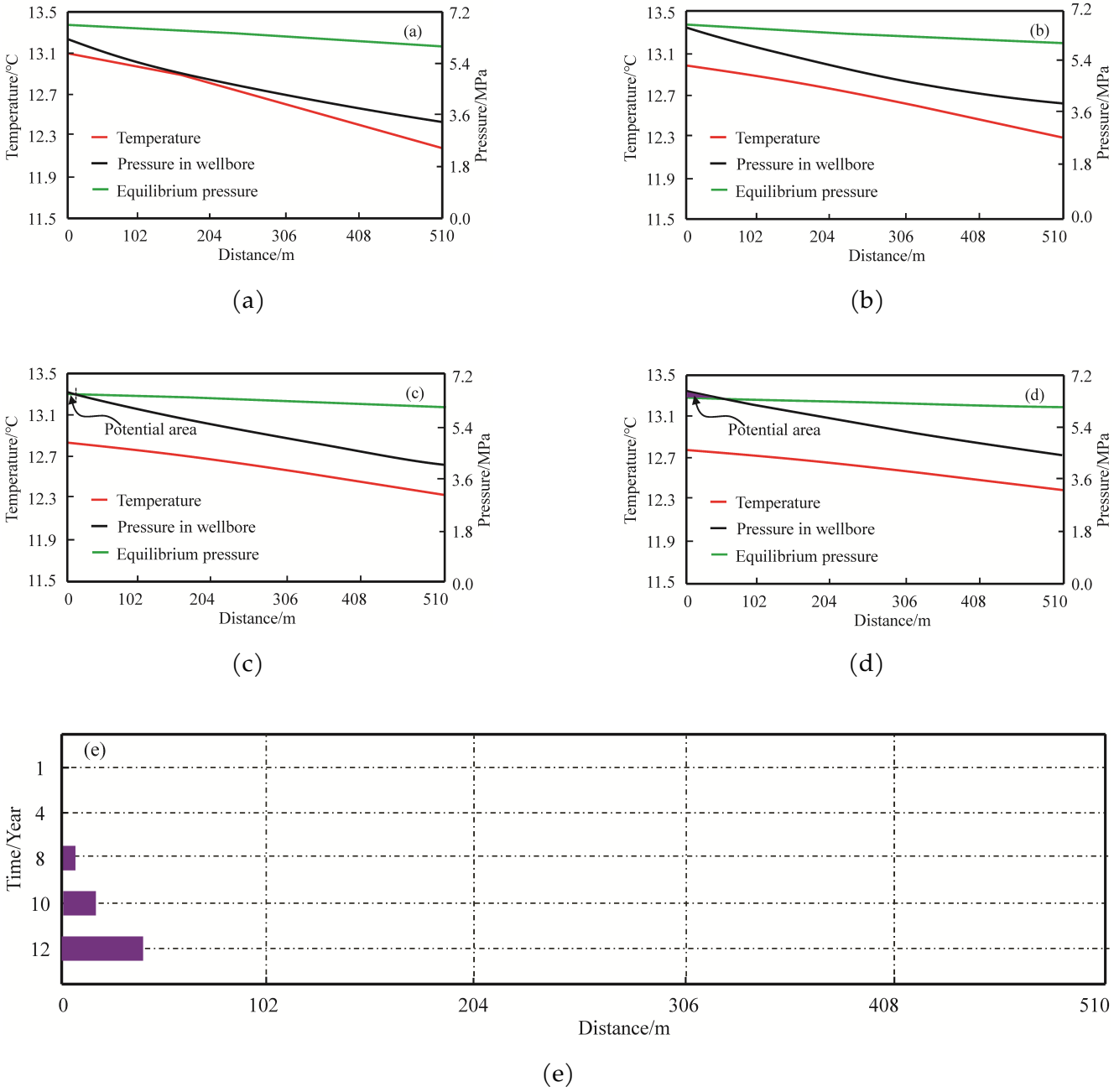

Figure 11. Risk evolution results of hydrate formation in riser. (a) 1 year; (b) 4 years; (c) 8 years; (d) 12 years; (e) Potential risk section.

4 Effect of methanol on equilibrium condition and hydrate formation risk

Methanol is the most commonly used inhibitor in practical applications at gas transmission stations and along pipelines. Despite concerns regarding toxicity, corrosiveness, and limited cost-effectiveness, methanol remains effective in lowering the hydrate formation temperature at relatively low expense. In this study, the effect of methanol, as an inhibitor, on phase equilibrium conditions and its role in reducing hydrate formation risk were investigated.

4.1 Experimental equipment and materials

Figure 12 presents the experimental system for investigating the influence of methanol on the phase equilibrium conditions of the gas mixture in Figure 7a. According to Figure 12, the experimental system is mainly consists of a high-pressure hydrate reactor, gas cylinder, stirrer, monitoring unit for temperature and pressure, injection system, and cold storage. The reactor, a thick-walled cylinder (10 cm internal radius, 30 cm height), is used to form hydrates of gas mixtures, methanol, and water under low-temperature, high-pressure conditions. The reactor wall is 1 cm thick

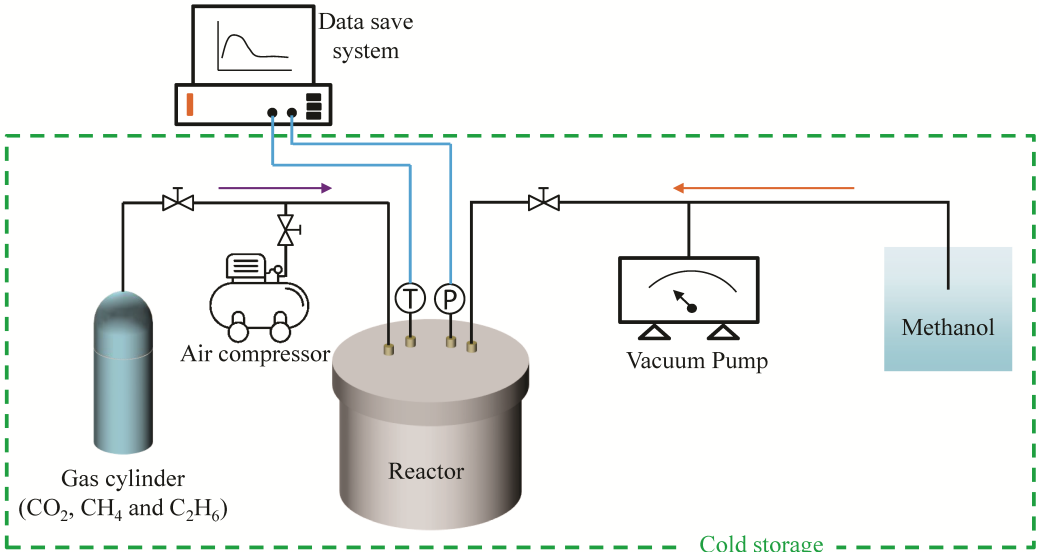

Figure 12. The experimental system.

and designed for pressures up to 120 MPa, ensuring reliable measurement of hydrate phase equilibrium pressures at normal temperatures. Four openings on the reactor's upper section allow for injection of gas and methanol, as well as placement of the temperature and pressure sensor. In addition, the measurement accuracies of the pressure and temperature sensors are ±20 kPa and ±0.1 °C, respectively. The cylinder stores a CO_2–CH_4–C_2H_6 mixture, with volume fractions as specified in Figure 7(a). Furthermore, the temperature and pressure sensors continuously transmit real-time data from the reactor to the storage system, enabling effective capture of experimental measurements at intervals of 5 minutes.

In this experiment, the main substances utilized are a mixture of gases and methanol. Among the experimental materials, the mixed gas was purchased from Henan Keyi Gas Co., Ltd., and its purity was 98%. Methanol, with a purity of 99%, was purchased from the China National Pharmaceutical Group.

4.2 Experimental method and scheme

It should be highlighted that the isothermal method was utilized for this experiment. The experimental procedure consisted of the following main steps:

(1) **Inspection of system airtightness**. Firstly, a certain amount of gas was injected into the experimental system, and the pressure within it was increased to about 2.0 MPa. At the same time, all valves on the pipelines were closed, and the reading of the pressure sensor was monitored. If the pressure sensor readings remain nearly constant, it indicates that the experimental system has good airtightness and subsequent experiments can proceed. Otherwise, the system must be repaired to meet the experimental requirements.

(2) **Injection of fluid and gas into reactor**. The experimental system is vacuumed, and a 500 mL methanol-water mixture is introduced into the high-pressure reactor via a vacuum pump. Then, the mixture of carbon dioxide, methane, and ethane is introduced into the high-pressure reactor using an air compressor until the pressure reaches the value specified in the experimental scheme. The pump and compressor are turned off, and the experimental stage for hydrate formation is commenced.

(3) **Hydrate formation experiment**. The ambient temperature is adjusted to the designated value (e.g., 2 °C) and maintained constant, while the mixer is activated with its speed controlled at approximately 700 rpm. Then, The pressure inside the reactor is gradually increased using an air compressor. At the same time, the data save system is initiated to capture the pressure and temperature measurements within the reactor. Following the experiment's completion, the pressure within the reactor and pipeline is discharged, and the obtained results are processed. By this method, the phase equilibrium conditions of the gas mixture presented in Figure 7(a) and the impact of methanol can also be evaluated.

In all experiments, the temperatures were designated as 0 °C, 3 °C, 6 °C, 9 °C, 12.0 °C, 15 °C, 18 °C, and 22.0 °C, respectively. Additionally, methanol was employed at concentrations of 2.5%, 5.0%, 7.5%, and 10%, respectively.

4.3 Experimental results

Figure 13 depicts the phase equilibrium curves for the mixture, established across a range of methanol concentrations. From Figure 13, it is evident that the phase equilibrium pressure of gas hydrates rises exponentially as the temperature is elevated from 273.15 K to 293.15 K. For a pure water system, when the temperature is elevated from 273.15 K to 293.15 K, the equilibrium pressure escalates from about 1.66 MPa to more than 16.90 MPa. This observation is consistent with the thermodynamic principle that hydrate formation is favored under conditions of low temperature and high pressure, which is true for all cases.

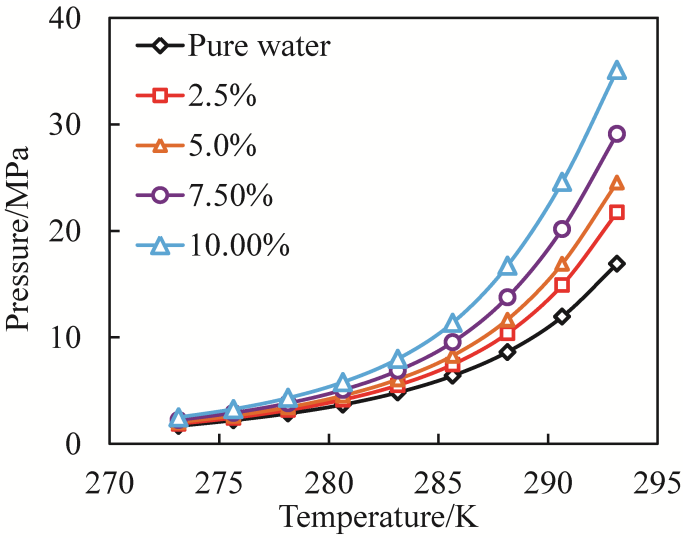

Figure 13. The experimental results.

With the methanol concentration raised from 0% to 10.0%, the phase equilibrium curve is incrementally displaced upward and leftward. At a constant temperature of 285.65 K, the phase equilibrium pressure of a pure water system is approximately 6.38 MPa. For methanol solution systems with 2.5%, 5.0%, 7.5%, and 10.0% concentrations, the phase equilibrium pressures are found to rise sequentially to approximately 7.44 MPa, 8.27 MPa, 9.54 MPa, and 11.36 MPa, respectively. The inhibition of hydrate formation by methanol is improved with rising methanol concentrations, and the magnitude of the offset is more evident at higher concentrations. This concentration-dependent behavior is attributed to the mechanism of methanol acting as a thermodynamic inhibitor. Strong hydrogen bonds are formed between methanol molecules and water, leading to the disruption of the hydrogen bonding network among water molecules through competitive interactions. The self-assembly of water molecules into cage-like crystal structures is thereby disrupted, resulting in an increased enthalpy change and a reduced entropy change during hydrate formation. As a result, the formation of mixed gas hydrates is deferred, leading to an increased range of the hydrate instability zone, illustrated in the bottom right corner of Figure 13. The findings demonstrate that hydrate-induced blockages in production system can be avoided through the proper injection of methanol. To facilitate numerical simulation, the hydrate phase equilibrium conditions at varying methanol concentrations (Figure 13) were fitted, as shown below.

$$\begin{cases} P = 4.12 \times 10^{-14} e^{0.1143T} \text{ (pure water)} \\ P = 6.03 \times 10^{-15} e^{0.1217T} \text{ (2.5\%)} \\ P = 3.06 \times 10^{-15} e^{0.1244T} \text{ (5.0\%)} \\ P = 1.11 \times 10^{-15} e^{0.1288T} \text{ (7.5\%)} \\ P = 2.95 \times 10^{-16} e^{0.1337T} \text{ (10.0\%)} \end{cases} \tag{10}$$

4.4 Optimization of methanol concentration

The injection of appropriate methanol concentrations into the production system during natural gas extraction from gas reservoirs is considered a critical strategy for suppressing hydrate formation and blockages in the wellbore and pipelines. However, the optimal methanol concentration remains to be determined. Therefore, a simulation analysis was carried out to assess the risk of hydrate formation in the wellbore and pipeline under different methanol concentrations.

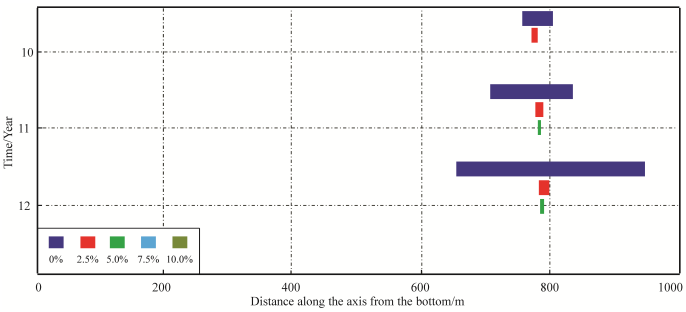

Figure 14. Section length of hydrate formation in wellbore when methanol concentration is different.

Figures 14, 15, and 16 present the simulation results of hydrate formation section lengths in the wellbore, flowline, and riser, respectively, under different methanol concentrations. From Figure 14, it can be seen that the presence of methanol in the wellbore fluid consistently leads to a significant decrease in the length of the wellbore section at risk of hydrate

formation, independent of the development cycle stage. When methanol at a concentration of 2.5% is injected into the wellbore fluid, a hydrate formation risk zone, approximately 15 to 20 meters in length, is observed throughout the entire gas production cycle. Upon elevating the methanol concentration to 5.0%, the presence of a hydrate formation risk stage across the entire wellbore is nearly absent. From the perspective of methanol's inhibitory on hydrate formation risk in wellbore, a methanol concentration below 5.0% is not recommended for the development design of this gas reservoir.

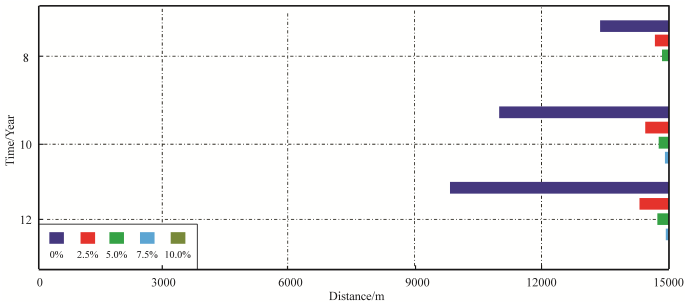

Figure 15. Section length of hydrate formation in flowline when methanol concentration is different.

From Figure 15, it is evident that methanol injection is highly effective in suppressing hydrate formation in the flowline and mitigating the risk of pipeline blockage. As shown in Figure 15, the risk section of hydrate formation in the flowline is shortened by more than 70% with a methanol concentration as low as 2.5%. With the methanol concentration raised to 5.0%, the length of the flowline section prone to hydrate formation is decreased by almost 90% or more. When the methanol concentration is increased to 7.5%, the presence risk of hydrate formation in the entire flowline is virtually eliminated. By comparing Figures 14 and 15, it is observed that methanol injection at the same concentration is more effective in mitigating the risk of hydrate formation in the wellbore than in the flowline. This is because the fluid temperature in the wellbore is higher, making the phase equilibrium conditions more sensitive to methanol injection. However, the fluid temperature in the flowline remains low, and the phase equilibrium conditions exhibit limited sensitivity to methanol injection. Based on the results regarding the impact of methanol on hydrate formation risk in the flowline, it is not advisable to reduce the methanol concentration below 7.5%.

According to Figure 16, the proper injection of methanol into the riser substantially lowers the risk of hydrate formation and considerably reduces the

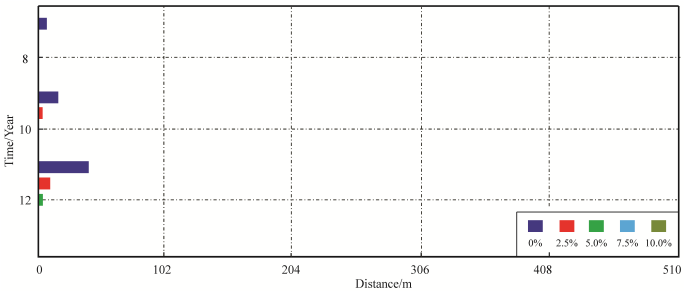

Figure 16. Section length of hydrate formation in riser when methanol concentration is different.

length of the potential risk section. After 8 years of the gas production, the riser section prone to hydrate formation is completely mitigated through the injection of methanol at a 2.5% concentration. By the tenth year of the gas production cycle, the injection of 2.5% methanol substantially shortens the riser section prone to hydrate formation, but the risk persists to some extent. To completely eliminate the risk of hydrate formation in the riser, it is necessary to further increase the methanol concentration as appropriate. For a gas production cycle of 12 years, the injected methanol concentration must be set to a minimum of 5.0%.

From Figures 14 to 16, it can be observed that methanol injection is highly effective in inhibiting hydrate formation in both wellbore and subsea gathering system. However, the investigation results reveal that the methanol concentration threshold required to completely eliminate risk of hydrate formation differs among the wellbore, flowline, and riser. It is well known that during the gas production process in a gas reservoir, the wellbore, riser, and flowline function as interconnected components of an integrated system. In this case, the determination of an optimized methanol injection concentration is necessary based on the simulation outcomes. In this study, the methanol concentration needs to be maintained at a minimum of 7.5%. In this way, the operational cost can be kept within an acceptable range while effectively mitigating the risks of hydrate formation and pipeline blockage in the production system.

5 Conclusions

The main conclusions are as follows:

(1) Over the 12-year gas production period, both the wellbore and the gathering system are subject to the risk of hydrate formation. Moreover, the formation of hydrates in the wellbore occurs later than in flowline and riser, but the extension speed of the risk section

length is faster. However, the length of the hydrate formation risk section in the flowline exceeds that of the other two investigation components. In any case, it is necessary to mitigate or eliminate these hydrate formation risk zones through appropriate engineering measures.

(2) The phase equilibrium conditions of hydrates in the studied gas mixtures are effectively modified by methanol. Specifically, as the concentration of injected methanol increases, the phase equilibrium curve shifts toward the upper-left region, thereby reducing the stable region. For a given temperature and pressure, the potential for hydrate formation is markedly decreased with the application of methanol. The injection of methanol is recognized as a critical engineering measure for ensuring efficient flow in the wellbore and gathering system during gas reservoir development for the investigation case herein.

(3) For this study, the risk section of hydrate formation in the wellbore, flowline, and riser are fully mitigated at methanol concentration thresholds of 5.0%, 7.5%, and 5.0%, respectively. On the whole, the lower limit for methanol concentration in the wellbore and gathering system should be designed at 7.5%.

Data Availability Statement

Data will be made available on request.

Funding

This work was supported without any funding.

Conflicts of Interest

The authors declare no conflicts of interest.

Ethical Approval and Consent to Participate

Not applicable.

References

[1] Zhai, S., Chauvet, C., Azarinezhad, R., Zeng, J., & Priyadarshi, A. (2015, June). Discussion of pipeline leakage and hydrate formation risks associated in deepwater natural gas pipelines. In *BHR International Conference on Multiphase Production Technology* (pp. BHR-2015). BHR.

[2] Babakhani, S. M., Bahmani, M., Shariati, J., Badr, K., & Balouchi, Y. (2015). Comparing the capability of artificial neural network (ANN) and CSMHYD program for predicting of hydrate formation pressure in binary mixtures. *Journal of Petroleum Science and Engineering, 136*, 78-87. [Crossref]

[3] Chen, D., & Sun, Z. (2023). Gas–Liquid Flow Pattern and Hydrate Risk in Wellbore during the Deep-Water Gas-Well Cleanup Process. *ACS omega, 8*(14), 12911-12921. [Crossref]

[4] Chen, H., Luo, M., Jiang, D., Wu, Y., Ma, C., Yu, X., ... & Zhang, Y. (2023). Research on the formation and plugging risk of gas hydrate in a deepwater drilling wellbore: A case study. *Processes, 11*(2), 488. [Crossref]

[5] Farhadian, A., Zhao, Y., Naeiji, P., Rahimi, A., Berisha, A., Zhang, L., ... & Zhao, J. (2023). Simultaneous inhibition of natural gas hydrate formation and CO2/H2S corrosion for flow assurance inside the oil and gas pipelines. *Energy, 269*, 126797. [Crossref]

[6] Ao, F., Qingchao, L., Qiang, L., Jingjuan, W., Fuling, W., & Chuanliang, Y. (2025). Numerical Simulation Investigation of Fracture Propagation Behavior Patterns and Sensitivity Factors of Oil Shale Reservoirs in the Xunyi Region Considering the Influence of Natural Fracture. *Geofluids, 2025*(1), 2762142. [Crossref]

[7] Feng, W., Li, D., Wang, G., & Song, Y. (2020). Wellbore Stability of a Deep-Water Shallow Hydrate Reservoir Based on Strain Softening Characteristics. *Geofluids, 2020*(1), 8891436. [Crossref]

[8] Gao, G., Zhang, G., Chen, G., Gang, W., Shen, H., & Zhao, K. (2018). Geochemistry of borehole cutting shale and natural gas accumulation in the deepwater area of the Zhujiang River Mouth-Qiongdongnan Basin in the northern South China Sea. *Acta Oceanologica Sinica, 37*(2), 44-53. [Crossref]

[9] Zhang, Y., Bai, C., Su, P., Xu, X., & Chang, Q. (2025). Predicting Gas Hydrate Saturation in Fine-Grained Sediments Using Machine Learning: A Case Study of the Shenhu Area in the Northern South China Sea. *Energy & Fuels*. [Crossref]

[10] Hao, Y., Yang, F., Wang, J., Fan, M., Li, S., Yang, S., ... & Xiao, X. (2022). Dynamic analysis of exploitation of different types of multilateral wells of a hydrate reservoir in the South China sea. *Energy & Fuels, 36*(12), 6083-6095. [Crossref]

[11] Zhu, L., Zhou, X., Sun, J., Liu, Y., Wang, J., & Wu, S. (2023). Reservoir classification and log prediction of gas hydrate occurrence in the Qiongdongnan Basin, South China Sea. *Frontiers in Marine Science, 10*, 1055843. [Crossref]

[12] Jiang, D., Yu, Y., Huang, Y., Meng, W., Su, J., & Gong, Z. (2021). Gas hydrate formation risk and prevention for the development wells in the Lingshui gas field in South China Sea. *Geofluids, 2021*(1), 9122863. [Crossref]

[13] Ju, G. S., Yan, T., Sun, X. F., Qu, J. Y., & Hu, Q. B. (2022). Evolution of gas kick and overflow in wellbore and formation pressure inversion method under the condition of failure in well shut-in during a blowout.

Petroleum Science, 19(2), 678-687. [Crossref]

[14] Bai, C., Wang, H., Li, Q., Zhang, Y., & Xu, X. (2024). Controls on Deep and Shallow Gas Hydrate Reservoirs in the Dongsha Area, South China Sea: Evidence from Sediment Properties. *Journal of Marine Science and Engineering, 12*(5), 696. [Crossref]

[15] Qingchao, L., Jingjuan, W., Qiang, L., Fuling, W., & Yuanfang, C. (2025). Sediment Instability Caused by Gas Production from Hydrate-Bearing Sediment in Northern South China Sea by Horizontal Wellbore: Sensitivity Analysis. *Natural Resources Research*, 1-33. [Crossref]

[16] Li, Q., Li, Q., & Han, Y. (2024). A numerical investigation on kick control with the displacement kill method during a well test in a deep-water gas reservoir: A case study. *Processes, 12*(10), 2090. [Crossref]

[17] Liao, Y., Sun, Q., Wang, Z., Sun, X., Lou, W., & Sun, B. (2022). Modeling of wellbore multiphase flow with free gas influx during horizontal drilling in marine hydrate reservoirs. *Journal of Natural Gas Science and Engineering, 97*, 104375. [Crossref]

[18] Liu, H., Lou, W., Li, H., Wang, Z., Gao, Y., Li, H., & Sun, B. (2024). A modified comprehensive prediction model for wellbore temperature-pressure field and liquid loading of gas wells. *Geoenergy Science and Engineering, 232*, 212452. [Crossref]

[19] Ma, Y., Hu, Z., Qu, Y., & Lu, G. (2013). Research on the characteristics and fundamental mechanism of a newly discovered phenomenon of a single moored FPSO in the South China Sea. *Ocean engineering, 59*, 274-284. [Crossref]

[20] Chen, X., Zhou, L., Zhang, C., Wang, S., Zhang, L., & Chen, J. (2022). Research Status and Future Development of Cooling Technologies for Green and Energy-Efficient Data Centers. *Strategic Study of Chinese Academy of Engineering, 24*(4), 94-104. [Crossref]

[21] Sajid, M. J., Yu, Z., & Rehman, S. A. (2022). The coal, petroleum, and gas embedded in the sectoral demand-and-supply Chain: Evidence from China. *Sustainability, 14*(3), 1888. [Crossref]

[22] Kelland, M. A. (2006). History of the development of low dosage hydrate inhibitors. *Energy & fuels, 20*(3), 825-847. [Crossref]

[23] Sloan Jr, E. D., & Koh, C. A. (2007). *Clathrate hydrates of natural gases*. CRC press. [Crossref]

[24] Sousa, A. M., Ribeiro, T. P., Pereira, M. J., & Matos, H. A. (2022). On the economic impact of wax deposition on the oil and gas industry. *Energy Conversion and Management: X, 16*, 100291. [Crossref]

[25] Sun, J., Ning, F., Liu, T., Li, Y., Lei, H., Zhang, L., ... & Jiang, G. (2021). Numerical analysis of horizontal wellbore state during drilling at the first offshore hydrate production test site in Shenhu area of the South China Sea. *Ocean Engineering, 238*, 109614. [Crossref]

[26] Sun, S., Ye, Y., Liu, C., Xiang, F., & Ma, Y. (2011). PT stability conditions of methane hydrate in sediment from South China Sea. *Journal of natural gas chemistry, 20*(5), 531-536. [Crossref]

[27] Jiang, D., Yu, Y., Huang, Y., Meng, W., Su, J., & Gong, Z. (2021). Gas hydrate formation risk and prevention for the development wells in the Lingshui gas field in South China Sea. *Geofluids, 2021*(1), 9122863. [Crossref]

[28] Yang, H., Li, J., Zhang, G., Zhang, H., Guo, B., & Chen, W. (2022). Wellbore multiphase flow behaviors during gas invasion in deepwater downhole dual-gradient drilling based on oil-based drilling fluid. *Energy Reports, 8*, 2843-2858. [Crossref]

[29] Yu, X., Gao, Y., Zhao, X., Yuan, H., Liu, L., & Sun, B. (2024). Research on heat transfer law of multiphase flow in wellbore under coexistence of overflow and lost circulation in deepwater drilling. *Case Studies in Thermal Engineering, 55*, 104103. [Crossref]

[30] Fu, J., Su, Y., Jiang, W., Xiang, X., & Li, B. (2020). Multiphase flow behavior in deep water drilling: The influence of gas hydrate. *Energy science & engineering, 8*(4), 1386-1403. [Crossref]

[31] Zhixin, W. E. N., Jianjun, W. A. N. G., Zhaoming, W. A. N. G., Zhengjun, H. E., Chengpeng, S. O. N. G., Xiaobing, L. I. U., & Tianyu, J. I. (2023). Analysis of the world deepwater oil and gas exploration situation. *Petroleum exploration and development, 50*(5), 1060-1076. [Crossref]

[32] Xu, Y., Guan, Z., Jin, Y., Pang, H., Liu, Y., Zhang, B., & Sheng, Y. (2017). Well control capacity-based risk analysis of gas cut in deepwater drilling. *Journal of Marine Science and Technology, 25*(2), 22. [Crossref]

[33] Zhang, L., Zhang, C., Huang, H., Qi, D., Zhang, Y., Ren, S., ... & Fang, M. (2014). Gas hydrate risks and prevention for deep water drilling and completion: A case study of well QDN-X in Qiongdongnan Basin, South China Sea. *Petroleum Exploration and Development, 41*(6), 824-832. [Crossref]

[34] Zhang, S. W., Shang, L. Y., Zhou, L., & Lv, Z. B. (2022). Hydrate deposition model and flow assurance technology in gas-dominant pipeline transportation systems: A review. *Energy & Fuels, 36*(4), 1747-1775. [Crossref]

[35] Zhang, W., Liang, J., Liang, Q., Wei, J., Wan, Z., Feng, J., ... & Chen, C. (2021). Gas hydrate accumulation and occurrence associated with cold seep systems in the northern South China Sea: An overview. *Geofluids, 2021*(1), 5571150. [Crossref]

[36] Zheng, J., Dou, Y., Li, Z., Yan, X., Zhang, Y., & Bi, C. (2022). Investigation and application of wellbore temperature and pressure field coupling with gas–liquid two-phase flowing. *Journal of Petroleum Exploration and Production Technology, 12*(3), 753-762. [Crossref]

[37] Zhi, J., Zhang, R., Qu, G., & Jiang, N. (2022).

Experimental Study on Stimulation of Horizontal Wells Filled with Film-Coated Gravel in Deep-Sea Bottom-Water Gas Reservoirs. *ACS omega, 7*(10), 9024-9032. [Crossref]

[38] Zhou, X., Mao, L., Guo, Z., & Gao, Y. (2024). Prediction of wellbore gas hydrate generation based on temperature-pressure coupling model in deepwater testing. *International Journal of Hydrogen Energy, 90*, 395-408. [Crossref]

Muyin Li is a master student at the School of Energy Science and Engineering, Henan Polytechnic University, Jiaozuo, China. His research interests include the efficient development of unconventional hydrocarbon resources (such as shale gas, natural gas hydrate, and deepwater oil and gas), theory and technology of mine disaster prevention and control. Li Muyin earned his Bachelor of Engineering from Henan Polytechnic University, Jiaozuo, China in 2023, and joined the School of Energy Science and Engineering at Henan Polytechnic University in the same year. (Email: livewood1999@163.com)

Junyi Liu is an undergraduate student at the School of Energy Science and Engineering, Henan Polytechnic University, Jiaozuo, China. Her major is New Energy Science and Engineering, mainly dedicated to the safe and efficient development of unconventional resources such as deepwater oil and gas, as well as the geothermal. She joined the School of Energy Science and Engineering at Henan Polytechnic University in 2022. (Email: liujunyi050709@163.com)

Yifan Xia is a master student at the School of Petroleum Engineering, China University of Petroleum (East China), Qingdao, China. His major is oil and gas well engineering, and he is mainly interested in the safe and efficient development of unconventional resources such as deepwater oil and gas, especially the safety design and control of drilling operations. He graduated at 2025, and joined the School of Petroleum Engineering at China University of Petroleum (East China) in the same year. (Email: Xiayifan_0919@163.com)